Progress In Electromagnetics Research M, Vol. 108, 127–137, 2022

Design and Analysis of a Compact UWB-MIMO Antenna with Four Notched Bands

Ling Wu[1, *], Xia Cao[2], and Bing Yang[3]

Abstract—In the paper, a very compact UWB-MIMO antenna with four rejected bands property is introduced and investigated. With a T-shape stepped stub on back ground, impedance bandwidth of 3–11 GHz and isolation of −15 dB are achieved. By etching four pairs of symmetrical L-formed slots into the radiators, four bands are isolated. With only a size of 21 mm × 27 mm, the proposed UWB-MIMO antenna system has low port coupling of −15 dB and wide working bandwidth of 3–11 GHz ($S_{11} \leq -10$ dB or VSWR ≤ 2) except 3.5 GHz WiMAX band, 5.3 GHz lower frequency band of WLAN, 5.8 GHz upper frequency band of WLAN, and 7.4 GHz X-band. Moreover, other characteristics, such as radiation patterns, antenna gain, antenna efficiency, and ECC (envelope correlation coefficient) are also studied.

1. INTRODUCTION

Ultra-wideband (UWB) technology has attracted much attention since Federal Communications Commission (FCC) officially designated 3.1–10.6 GHz frequency band for UWB commercial purposes [1]. Due to its outstanding advantages of low power, high data rata, and strong anti-jamming UWB technology is regarded as an excellent choice in some wireless communications, such as imaging systems, ranging, and positioning. Multiple-input-multiple-output (MIMO) technology is another promising technology, which can greatly improve data rate without increasing transmission power and bandwidth. Incorporating MIMO technology into UWB, UWB-MIMO can make full use of their advantages and provide more than 1 Gb/s data rate [2]. Generally, in terminal communication system antenna must be provided with a small size. However, in limited antenna space, keeping high port isolation or low mutual coupling (MC) is a big challenge for UWB-MIMO systems. Another challenge is electromagnetic interference. Some wireless communication systems coexisting with UWB in 3.1–10.6 GHz will bring unwanted signal interference to UWB, for example WiMAX band (3.5 GHz) WLAN band (5.5 GHz) and X-band (7.5 GHz). In this regard, the study of UWB-MIMO antennas with properties of notched band (NB) and low MC is conducive.

Some techniques of developing NBs for UWB antennas have been introduced in [4–13]. A U-shaped slot, an elliptical slot, and two pairs of quarter-wavelength stubs are used to generate a notch in [3–5], respectively. Refs. [6–8] realized dual NBs, in which a slot and EBG structure was used in [6], an I-shaped and C-shaped stubs in [7], a C-shaped slot and complementary split-ring resonator (CSRR) in [8]. Triple NBs were produced in [9, 10]. Mirrored Γ-shape slots, L-shape slots, and a bent C-shape stub were used for triple NBs in [9] and a hook-shaped slot and two strips in [10]. Four CSRR slots and four U-slots offered a good choice to reject four bands in [11, 12], respectively. Placing an inverted U-shaped slot and C-shaped slots, quintuple NBs were attained in [13].

It is a big challenge to design a compact UWB-MIMO antenna which can be applied to portable wireless systems, as closely spaced radiators cause high mutual coupling. Some decoupling technologies

Received 21 November 2021, Accepted 30 December 2021, Scheduled 18 February 2022
* Corresponding author: Ling Wu (ruochen143abc@163.com).
[1] School of Physics and Electronic Information Engineering, Hubei Engineering University, Hubei, China. [2] Wuhan Qingchuan University, Wuhan, Hubei, China. [3] Wuhan Polytechnic University, Wuhan, Hubei, China.

have also been reported in [14–32], such as a hybrid method of CSRR and ground stubs in [14], TH-like parasitic structure in [15], defected ground structure (DGS) in [16], neutralization line in [17], polarization diversity in [18], connected ground system in [19], and multi-slot isolator in [20]. The UWB-MIMO antennas in [21–32] offered multiple NBs. In [21], an H-shaped slot was curved in ground plane to improve port isolation, and an open stub was etched on radiator to avoid 5.5 GHz band. Ref. [22] employed a U-shaped slot to get 5.5 GHz stopband and a T-shape stub for port isolation. Ref. [23] adopted a T-shape ground stub as a decouple element and an L-shape strip to suppress 4.17 GHz band. Arranging two elements at a distance of $\lambda/8$, high isolation was obtained in [24]. Two U-shaped slots were used for two notches. Ref. [25] utilized two slots to improve isolation. With trident-shape metal strips, 5.7 GHz band and 8 GHz band were stopped. In [26], an elliptical T-shape stub helped diminish MC, and a G-shape stub made dual notched bands. In [27] and [28], dual NBs were achieved by inserting two L-shaped slits, and −22 dB isolation was obtained by L-shaped ground plane in [27]. −15 dB isolation was observed by a T-shape stub in [28]. With EBGs, [29] and [30] attained triple stopbands. Strips and slotted ground plane in [29] and F-shaped stubs in [30] can help alleviate MC. In [31], two slots and an EBG element were used in a 4-port UWB-MIMO antenna to stop three bands, and perpendicular placement of radiators and a parasitic strip helps reduce MC. Four rings with rectangular split bricks were used in [32] for quad stopbands and a ground stub for suppressing MC.

With a small profile volume of 21 mm × 27 mm × 0.8 mm, a quad NB UWB-MIMO antenna which covers 3.1–10.6 GHz UWB band is studied. The system comprises two identical half-rectangle radiators which both cut off a bevel edge for better impedance bandwidth. Four pairs of symmetrical L-formed slots are inserted to each radiator to filter WiMAX frequency band (3.5 GHz), lower band of WLAN (5.3 GHz), upper band of WLAN (5.8 GHz), and X-band (7.4 GHz). A T-shape stepped stub on the back ground not only expands impedance bandwidth but also alleviates MC. Having a very small size of 21 mm × 27 mm and −15 dB isolation, the introduced UWB-MIMO antenna realizes four NBs in 3–11 GHz band, which is a novel contribution of the design.

2. ANTENNA DESIGN

2.1. Antenna Design

Figure 1 shows the sketch and manufactured prototype of the proposed antenna. The system was printed on a 21 × 27 × 0.8 mm^3 loss FR4 PCB substrate (dielectric constant $\varepsilon_r = 4.4$, loss tangent

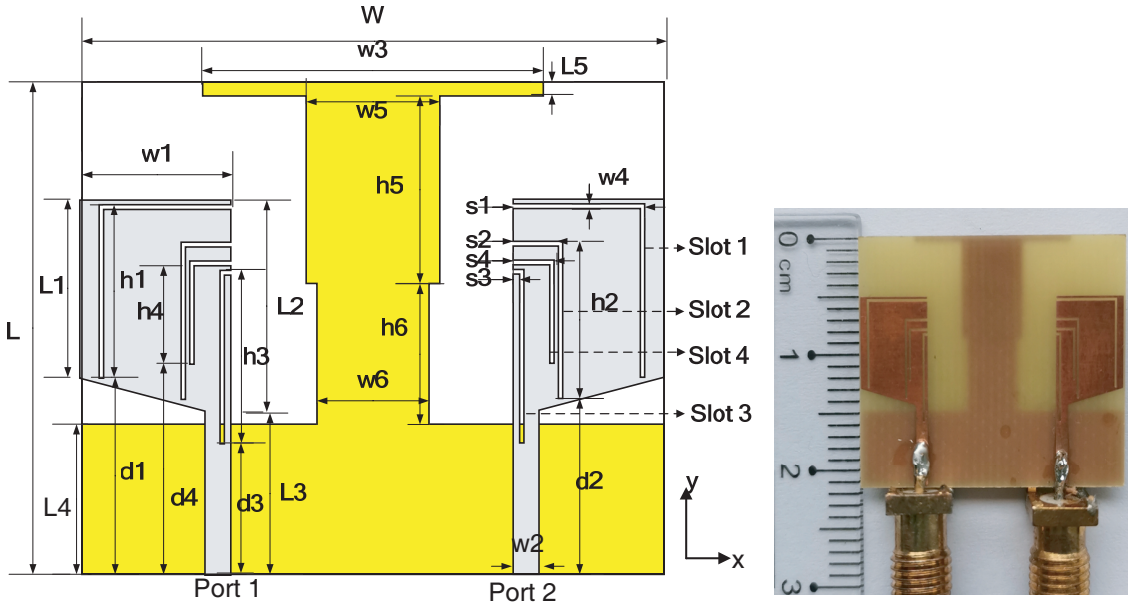

Figure 1. (a) Schematic of proposed antenna and (b) manufactured prototype.

= 0.025). On the basis of half-cutting methodology [33], two identical half-rectangle radiators were cut off and then placed side by side in front of the microstrip-fed UWB-MIMO system. Each radiator was cut off a bevel edge for better impedance bandwidth. A T-shape stepped stub on the back ground was adopted for decoupling and expanding impedance bandwidth. Thus, the size of antenna is reduced and only occupies 21 mm × 27 mm.

Aiming to obtain four stopbands, symmetrical L-formed slots (named Slot1, Slot2, Slot3, Slot4) were inserted to each radiator step by step. These slots are similar to the design in [31], and the difference is that the former are etched on the half-rectangle patch and the latter etched on microstrip feeder. Fig. 2 shows the step-by-step design processes.

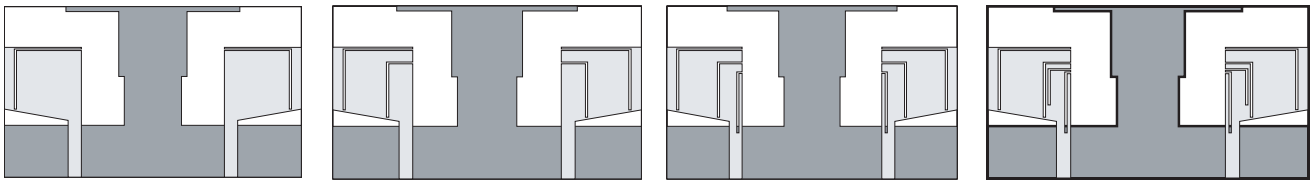

Figure 2. The step-by-step design processes; (a) Ant-A; (b) Ant-B; (c) Ant-C; (d) Proposed.

Figure 3 shows simulated S-parameters of the above four antennas. From Fig. 3, it is obvious that Slot1, Slot2, Slot3, Slot4 are responsible for notching 3.5 GHz, 5.3 GHz, 5.8 GHz, and 7.4 GHz, respectively. In Figs. 3(a)–(d), it can also be observed that S_{21} is < -15 dB, and these four L-formed slots have little impact on S_{21}.

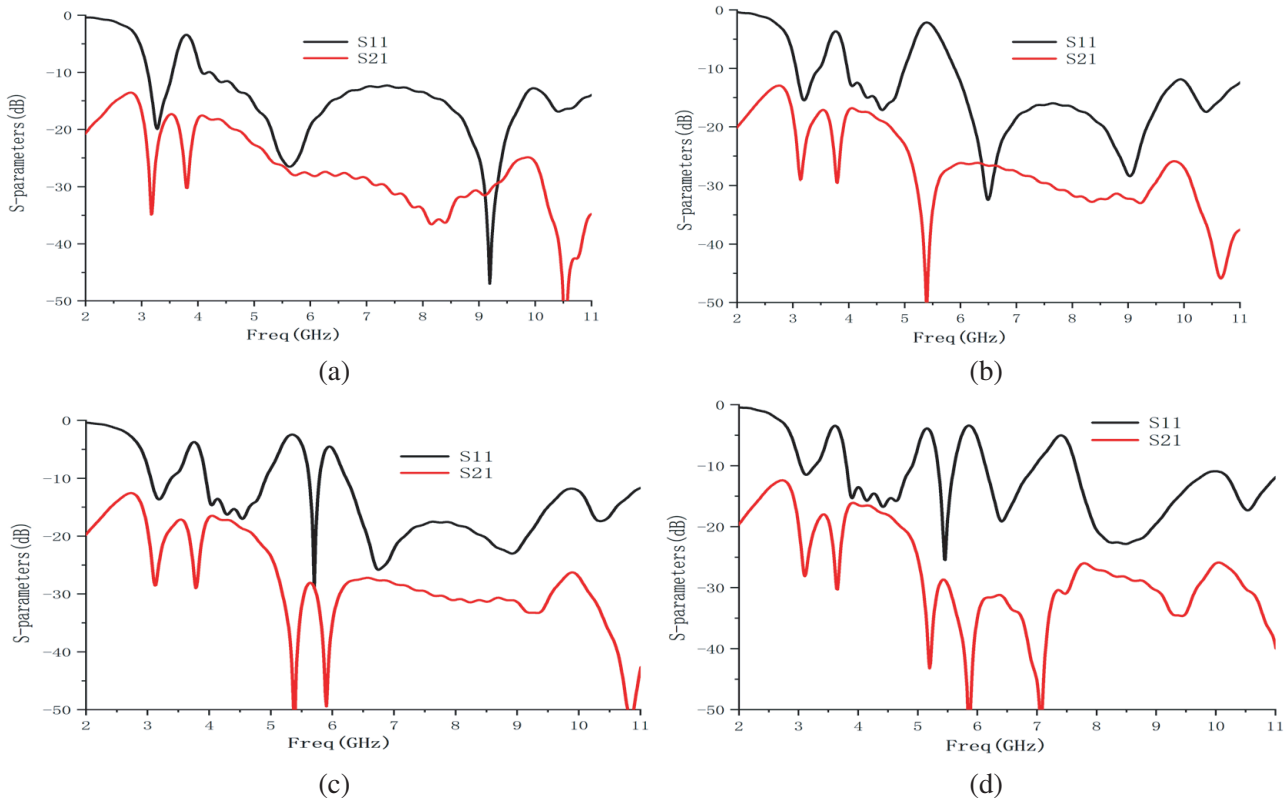

Figure 3. Simulated S-parameters of Ant-A, Ant-B, Ant-C and Proposed; (a) Ant-A; (b) Ant-B; (c) Ant-C; (d) Proposed.

Using simulation software of CST Microwave Studio 2018 and through multiple simulations, the final optimum parameters are adopted and listed in Table 1.

Table 1. Parameters of the proposed antenna.

Parameter	mm	Parameter	mm	Parameter	mm
W	27	$s2$	2.3	$s4$	1.9
L	21	$d2$	7.5	$d4$	9
$w1$	7	$w3$	15.8	$w5$	6.2
$L1$	7.6	$L3$	7	$w6$	5.2
$h1$	7.2	$h3$	7.2	$L5$	0.6
$s1$	6.1	$s3$	0.5	$h5$	9.2
$d1$	8.4	$d3$	5.4	$h6$	6
$w2$	1.2	$w4$	0.2		
$L2$	9	$L4$	6.4		
$h2$	6.5	$h4$	4.2		

2.2. Effect of the T-Shape Stepped Stub

The T-shape stepped stub plays a vital role in this design, because it accounts for wider impedance matching and also helps eliminate MC. Fig. 4 exhibits design process of the back plane. In Fig. 4(a), a common ground is adopted, named Ant-1. In Fig. 4(b), a T-shape stepped stub is extruded from middle of the back ground, named Ant-2. Because the two radiators are identical, S_{11} and S_{21} are the same as S_{22} and S_{12}.

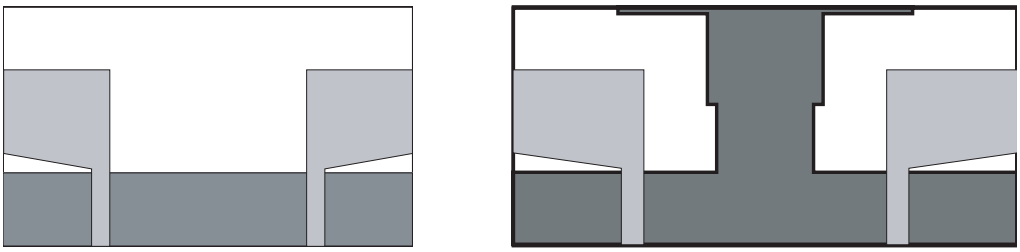

Figure 4. Design process of the back plane; (a) Ant-1; (b) Ant-2.

Figure 5 shows simulated S_{11} and S_{21} of Ant-1 and Ant-2. In Fig. 5(a), at frequency band less than 5.2 GHz, S_{11} value is greater than -10 dB for Ant-1. However, low cut-off frequency ($S_{11} < -10$ dB) is 3.1 GHz for UWB. In Ant-2, a T-shape stepped stub was extruded. Inclusion of the T-shape stepped stub excites a resonance at 3.4 GHz, which reduces the cut-off frequency to 3 GHz, as shown by the red line in Fig. 5(a). It greatly improved impedance matching in the low frequency band, so that 3.1–10.6 GHz UWB was covered. However, Ant-1 has poor isolation, because S_{21} is above -15 dB at low frequency band, which is plotted in Fig. 5(b). After adopting the T-shape stepped stub, S_{21} is below -15 dB in the whole UWB which can meet the requirements of MIMO system.

To depict decoupling function of the T-shape stepped stub, Fig. 6 shows current density at 3.4 GHz, 5.45 GHz, and 9.4 GHz. In Fig. 6(a), without any decoupling element, a great deal of electrical current flowed to port 2 uninterrupted. However, in Figs. 6(b)–(d), at three resonant frequencies, the T-shape stepped stub trapped most of the current, and only small current flowed to port 2. So MC was weakened greatly.

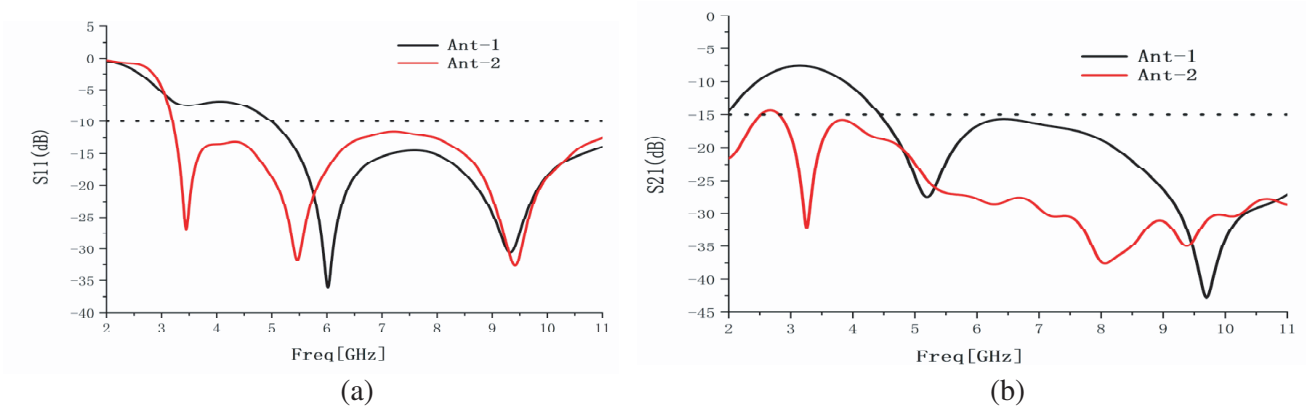

Figure 5. Simulated S parameters: (a) S_{11}; (b) S_{21}.

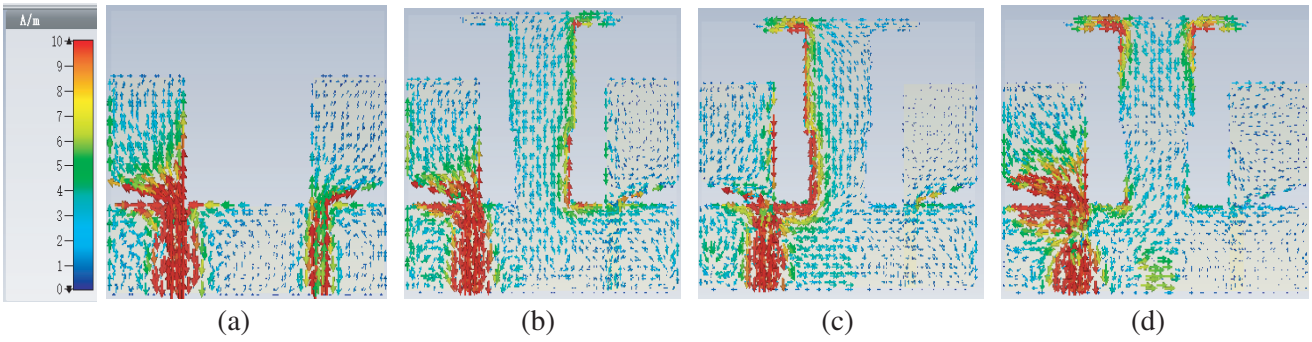

Figure 6. Current distributions when port1 is excited; (a) 3.4 GHz of Ant-1; (b) 3.4 GHz of Ant-2; (c) 5.45 GHz of Ant-2; (d) 9.4 GHz of Ant-2.

2.3. Effects of Four Pairs of Symmetrical L-Formed Slots

Compared with adding extra filtering equipment, etching slots or slits on antenna is a simple and effective notch technology. To yield four stopbands mentioned above, four pairs of symmetrical L-formed slots are etched on each radiator. We adjust the length of corresponding slot (L_t) to about a quarter of λ_g which is the wavelength corresponding to center frequency of each notch (f_{nb}), and can be expressed by formula (1).

$$\lambda_g = \frac{\lambda_0}{\sqrt{\varepsilon_{eff}}} = \frac{c}{f_{nb}\sqrt{\varepsilon_{eff}}} \tag{1}$$

Then L_t is derived by formula (2).

$$L_t = \frac{\lambda_g}{4} = \frac{c}{4f_{nb}\sqrt{\varepsilon_{eff}}} \tag{2}$$

where c is the light speed of 3×10^8 m/s, and $\varepsilon_{eff} \approx \frac{\varepsilon_r+1}{2}$ is the effective dielectric constant.

These slots seem as a quarter-wavelength impedance transformer, which causes impedance mismatch at each stopband. Calculated and optimized simulation L_t are shown in Table 2. Taking Slot1 as an example, since Slot1 leads to 3.5 GHz NB, its calculated length L_{t1} was 13 mm. But its simulated value was $s1 + h1 = 13.3$ mm. Te error between the two is 0.3 mm. From Table 2, there is little error which demonstrates the feasibility of the design.

Then some significant parameters were chosen to observe their effect on S_{11}, which are shown in Fig. 7. If one parameter is adjusted, the other parameters remain unchanged. Because Slot1, Slot2, Slot3, and Slot4 are similar in structure, similar phenomenon will occur when analyzing the influence of parameters on S_{11}. Only Slot4 is analyzed here. In Table 2, Lt4 of Slot4 is equal to $s4+h4$. In Fig. 7(a),

Table 2. Calculated and simulated values of each NB structure.

L_t	NB (GHz)	Calculated value (mm)	Simulated value (mm)	Error (mm)
L_{t1} of Slot1	3.5	13	13.3 ($= s1 + h1$)	0.3
L_{t2} of Slot2	5.3	8.6	8.8 ($= s2 + h2$)	0.2
L_{t3} of Slot3	5.8	7.87	7.7 ($= s3 + h3$)	0.17
L_{t4} of Slot4	7.4	6.17	6.1 ($= s4 + h4$)	0.07

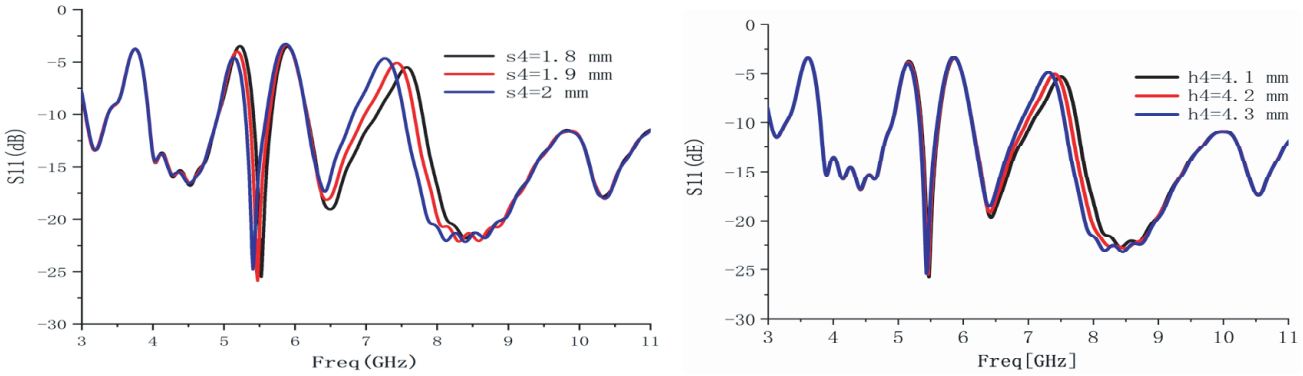

Figure 7. Simulated S_{11}: (a) effect of $s4$; (b) effect of $h4$.

when $s4$ was added, total length L_{t4} was increased, then the fourth NB moved to lower frequency band. This phenomenon can also be drawn from formula (2). Meanwhile, the amplitude increases with the increase of $s4$. In Fig. 7(b), changing $h4$ from 4.1 mm to 4.3 mm, the fourth NB moved slightly to the left. Thus $s4$ and $h4$ are key parameters in the formation of 7.4 GHz NB.

Figure 8 describes current density distributions for further understanding the formation mechanism of NBs. Obviously, in Figs. 8(a)–(d), strong electricity was trapped by corresponding slot at each NB, and energy cannot be sent out effectively. Moreover, on each slot, the current is the strongest at the place closest to the feeder, and then gradually decreases. We can regard each slot as a quarter-wavelength converter, which transformed nearly zero impedance (strongest current) to high impedance (weakest current). The impedance mismatch caused the formation of NB.

3. RESULTS AND DISCUSSIONS

The proposed quad-notched band UWB-MIMO antenna was manufactured which is shown in Fig. 1(b). Agilent E8362B network analyzer was used to measure S-parameters. When a port was excited, the other port was loaded with a 50 ohm load.

Figure 9(a) shows S_{11} of simulation and measurement. It was found that from 3 to 11 GHz, S_{11} values are < -10 dB, except four NBs at 3.3–3.7 GHz, 4.9–5.5 GHz, 5.6–6.2 GHz, and 7–7.6 GHz. Simulated and measured S_{21} are compared in Fig. 9(b). Measured S_{21} maintains < -15 dB in the whole 3.1–10.6 GHz UWB, and in most frequency bands, S_{21} is less than -20 dB. Thus high isolation was achieved, which indicates that the antenna meets -15 dB MIMO criterion. Moreover, in Fig. 9, the trends of the two curves are roughly the same except for some deviation, which is due to tolerable factors like test environment, welding effect, and substrate fabrication error.

Normalized far-field radiation patterns of E plane and H plane are shown in Fig. 10 for port 1 at four resonant frequencies of 3.2 GHz, 5.45 GHz, 6.4 GHz, and 10.3 GHz. As plotted in Fig. 10(a), in E plane (yoz plane), the antenna has quasi-omnidirectional pattern instead of '8' shape. This phenomenon

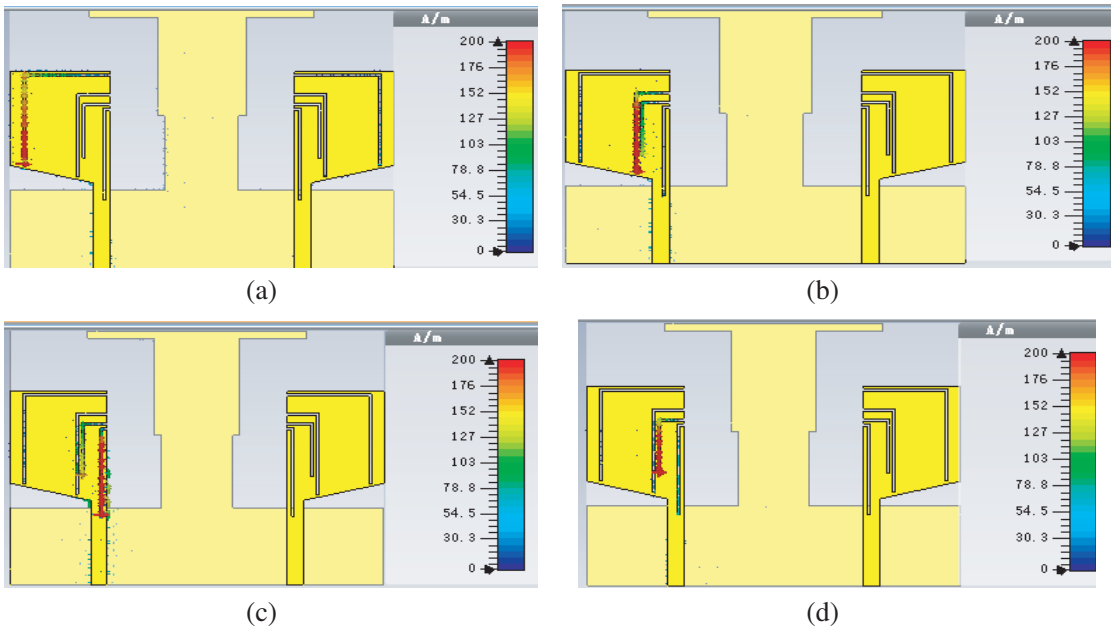

Figure 8. Surface current distributions at four NBs for port 1: (a) 3.5 GHz; (b) 5.3 GHz; (c) 5.8 GHz; (d) 7.4 GHz.

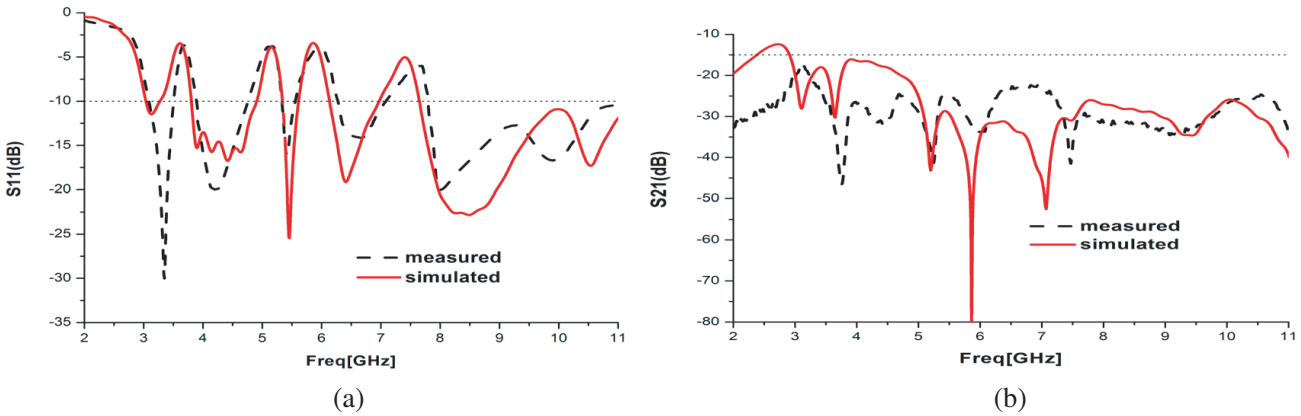

Figure 9. Simulated and measured S-parameters of the proposed antenna; (a) S_{11}; (b) S_{21}.

is attributed to electric current on the protruded T-stepped stub resulting in null drift [34]. It is clear that in H plane (xoz plane), as shown in Fig. 10(b), quasi-omnidirectional radiation performance is observed.

Figure 11 shows far-field radiation efficiency and antenna gain when port 1 is excited. Except four minimums at 3.5 GHz band, 5.3 GHz band, 5.8 GHz band, and 7.4 GHz band, stable gain was observed, and radiation efficiency was above 70% in the working band.

Moreover, envelope correlation coefficient (ECC) was analyzed for better evaluating diversity performance of a MIMO antenna. The calculation of ECC for MIMO system is based on far-field parameters [18]:

$$\rho_e = \frac{\left|\iint \left[F_1(\theta,\varphi)\cdot F_2(\theta,\varphi)\right] d\Omega\right|^2}{\iint \left|F_1(\theta,\varphi)\right|^2 d\Omega \iint \left|F_2(\theta,\varphi)\right|^2 d\Omega} \tag{3}$$

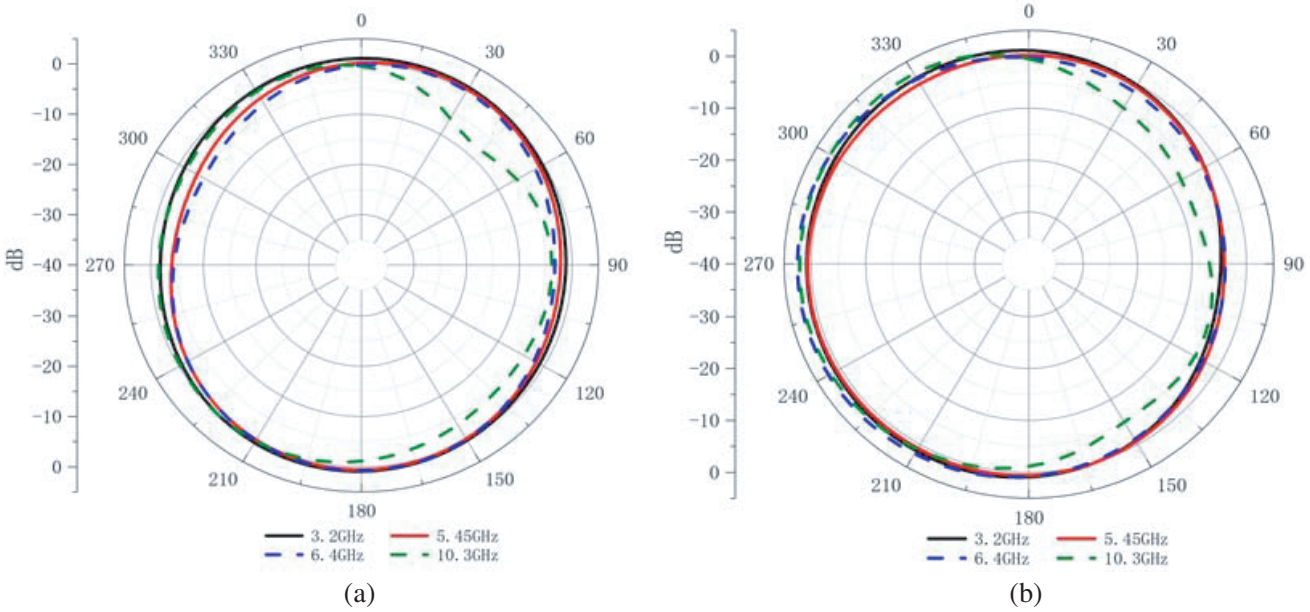

Figure 10. Normalized far-field radiation patterns for Port 1: (a) E plane and (b) H plane.

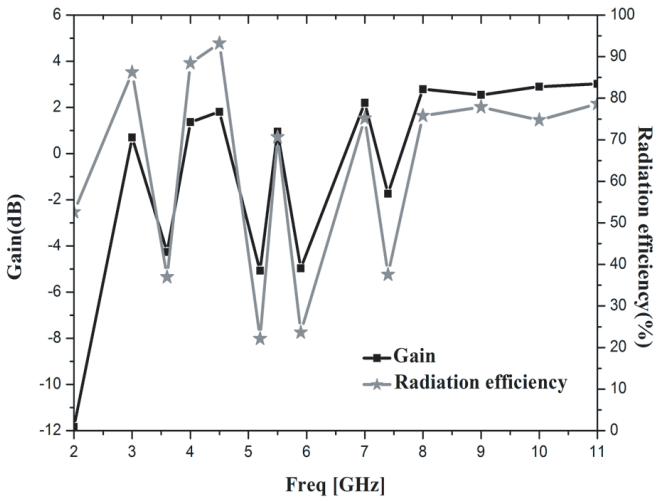

Figure 11. Peak gain and Radiation efficiency.

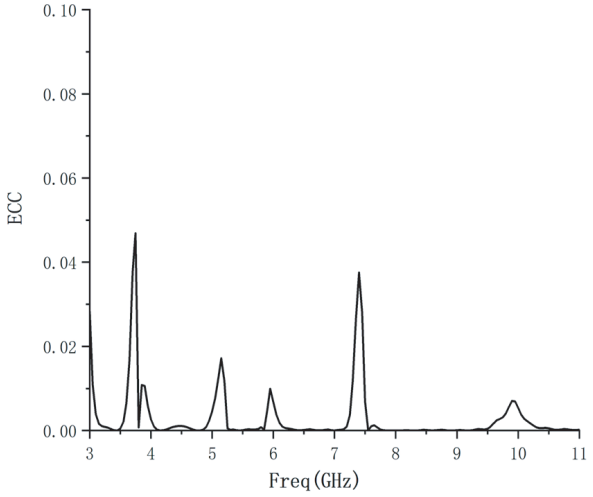

Figure 12. ECC using far-field parameters.

Here $F_i(\theta, \varphi)$ is a 3-D far-field pattern when port i is excited. From Fig. 12, ECC values are less than 0.05 in the entire working band of UWB.

In the end, the proposed design is compared with other reported UWB-MIMO antennas in Table 3. Antennas in [14, 20–23, 25–28] have a relatively small area, but the number of NB is no more than two. TH-like element, DGS, and Neutralization line were used for achieving isolation of −20 dB in [15], −15 dB in [16], and −22 dB isolation in [17], respectively. Without decoupling structure, MC is attenuated in [18] and [24]. However, the antenna in [24] had relatively large size and −12 dB isolation. To suppress MC, connected ground system was applied in four-port UWB-MIMO antenna in [19]. With only a size of 30 mm × 20 mm and a novel multi-slot isolator, the antenna in [20] has −20 dB isolation. Antennas in [29–32] achieved triple NBs. However, both [29] and [30] occupied big space. The 4-port antenna system in [31] was only 34 mm × 34 mm in size. With a size of 50 mm × 31 mm, [32] realized four NBs. From Table 3, the proposed design not only implements four NBs but also has very small profile.

Table 3. Comparison of reported UWB-MIMO antennas.

Ref.	NB number	Isolation (dB)	NB technique	Decoupling technique	Size (mm^2)	Port number
[14]	-	−20	-	CSRR and ground stubs	$29 \times 23 = 667$	2
[15]	-	−20	-	TH-like	$46 \times 32.6 = 1499.6$	2
[16]	-	−15	-	DGS	$30 \times 40 = 1200$	2
[17]	-	−22	-	neutralization line	$35 \times 33 = 1155$	2
[18]	-	−15	-	vertical placement	$55 \times 55 = 3025$	2
[19]	-	−15	-	connected ground system	$45 \times 66 = 2970$	4
[20]	-	−20	-	multi slot isolator	$30 \times 20 = 600$	2
[21]	1	−20	an open stub	H-shaped slot	$22 \times 28 = 616$	2
[22]	1	−15	U-shaped slot	T-shape stub	$20 \times 36 = 720$	2
[23]	1	−20	L-shaped metal strip	T-shape ground stub	$18 \times 36 = 648$	2
[24]	2	−12	U-shaped slots	keeping radiating element $\lambda/8$ apart	$25.7 \times 47 = 1207.9$	2
[25]	2	−20	trident-shape metal strips	a narrow slot	$22 \times 26 = 572$	2
[26]	2	−20	a G-shape stub	elliptical T-shape stub	$18 \times 36 = 648$	2
[27]	2	−22	L-shaped slits	L-shaped strips	$18 \times 34 = 612$	2
[28]	2	−15	L-shaped slits	T-shape stub	$26 \times 28 = 728$	2
[29]	3	−15	EBGs	Strips and slotted ground plane	$64 \times 45 = 2880$	2
[30]	3	−20	EBGs	F-shaped stub	$30 \times 44 = 1320$	2
[31]	3	−15	slots and EBG	perpendicular placement and a parasitic strip	$34 \times 34 = 1156$	4
[32]	4	−15	four rings with rectangular split bricks	a ground stub	$50 \times 31 = 1550$	2
This work	4	−15	four L-shape slots	a T-shape stepped stub	$21 \times 27 = 567$	2

*NB denotes notched band

4. CONCLUSION

With very compact size of $21 \times 27\,mm^2$, a quad-notched band UWB-MIMO antenna was constructed and analyzed. Inserting four pairs of symmetrical L-formed slots to each radiator, four NBs of 3.5 GHz, 5.3 GHz, 5.8 GHz, and 7.4 GHz were observed in operating band of 3–11 GHz. With a T-shape stepped stub, both isolation of −15 dB and 3–11 GHz impedance matching are guaranteed. Moreover, other characteristics such as stable gain, acceptable far-filed radiation patterns, and ECC of no more than 0.05 are obtained, indicating that the proposed antenna is a good choice for UWB applications.

ACKNOWLEDGMENT

This work are supported by Scientific Research Project of Hubei Provincial Department of Education (D20212702, Q20211608) and Natural Science Foundation of Xiao Gan China (Grant Nos. XGKJ2021010001). The authors are grateful for technical help provided by electromagnetic microwave laboratory of Hua Zhong Normal University.

REFERENCES

1. "Federal Communications Commission Revision of Part 15 of the Commission's Rules Regarding Ultra-Wideband Transmission System from 3.1 to 10.6 GHz," *FEDERAL Communications Commission*, 98–153, FCC, ETDocket, Washington, DC, 2002.
2. Kaiser, T., Z. Feng, and E. Dimitrov, "An overview of ultra-wideband systems with MIMO," *Proc. IEEE*, 285–312, 2009.
3. Debab, M. and Z. Mahdjoub, "Single band notched characteristics UWB antenna using a cylindrical dielectric resonator and U-shaped slot," *J. Microwaves, Optoelectron. Electromagn. Appl.*, Vol. 17, No. 3, 340–351, 2018.
4. Babu, K. J., B. K. Kumar, B. S. Rao, and A. M. Varaprasad, "Design of a compact elliptical slot printed UWB antenna with band-notched characteristic," *International Journal of Electronics Letters*, Vol. 7, No. 4, 448–457, 2019.
5. Zhang, J., T. Chen, L. Hua, and W. Wang, "A compact differential-fed UWB antenna with band-notched characteristics," *Progress In Electromagnetics Research M*, Vol. 83, No. 8, 171–179, 2019.
6. Kadam, A. A. and A. A. Deshmukh, "Pentagonal shaped UWB antenna loaded with slot and EBG structure for dual band notched response," *Progress In Electromagnetics Research M*, Vol. 95, 165–176, 2020.
7. Rabah, W. A., S. A. Ibrahim, J. B. Kamili, and M. S. Muntasir, "A compact CPW-fed UWB antenna with dual-band notched characteristics for WiMAX/WLAN applications," *ACES Journal*, Vol. 36, No. 2, 145–151, 2021.
8. Sharma, N., S. S. Bhatia, V. Sharma, and J. S. Sivia, "An octagonal shaped monopole antenna for UWB applications with band notch characteristics," *Wireless Personal Communications*, Vol. 111, 1977–1997, 2020.
9. Kadam, A. A. and A. A. Deshmukh, "Compact triple band notched pentagonal shaped UWB antenna loaded with slots and parasitic resonator," *Journal of Microwaves, Optoelectronics and Electromagnetic Applications*, Vol. 20, No. 2, 320–333, 2021.
10. Cui, L., H. Liu, C. Hao, and X. Sun, "A novel UWB antenna with triple band-notches for WiMAX and WLAN," *Progress In Electromagnetics Research Letters*, Vol. 82, 101–106, 2019.
11. Kalyan, R., K. T. V. Reddy, and K. P. Priya, "Compact CSRR etched UWB microstrip antenna with quadruple band refusal characteristics for short distance wireless communication applications," *Progress In Electromagnetics Research Letters*, Vol. 82, 139–146, 2019.
12. Mewara, H. S., D. Jhanwar, M. M. Sharma, and J. K. Deegwal, "A printed monopole ellipzoidal UWB antenna with four band rejection characteristics," *Int. J. Electron. Commun. (AEÜ)*, Vol. 83, 222–232, 2018.
13. Mewaraa, H. S., J. K. Deegwala, and M. M. Sharma, "A slot resonators based quintuple band-notched Y-shaped planar monopole ultra-wideband antenna," *Int. J. Electron. Commun. (AEÜ)*, Vol. 83, 470–478, 2018.
14. Khan, M. S., A. D. Capobianco, S. M. Asif, et al., "A compact CSRR-enabled UWB diversity antenna," *IEEE Antennas and Wireless Propagations Letters*, Vol. 16, 808–812, 2017.
15. Kumar, R., R. V. S. R. Krishna, and N. Kushwaha, "Design of a compact MIMO/diversity antenna for UWB applications with modified TH-like structure," *Microw. Opt. Technol. Lett.*, Vol. 58, No. 5, 1181–1187, 2016.
16. Deng, J. Y., L. X. Guo, and X. L. Liu, "An ultrawideband MIMO antenna with a high isolation," *IEEE Antennas and Wireless Propagations Letters*, Vol. 15, 182–185, 2016.

17. Zhang, S. and G. F. Pedersen, "Mutual coupling reduction for UWB MIMO antennas with a wideband neutralization line," *IEEE Antennas and Wireless Propagation Letters*, Vol. 15, 166–169, 2016.
18. Addepalli, T., A. Desai, I. Elfergani, et al., "8-port semi-circular arc MIMO antenna with an inverted L-strip loaded connected ground for UWB applications," *Electronics*, Vol. 10, No. 12, 1476, 2021.
19. Desai, A., M. Palandoken, K. Jayshri, et al., "Wideband flexible/transparent connected-ground MIMO antennas for sub-6 GHz 5G and WLAN applications," *IEEE Access*, Vol. 9, 147003–147015, 2021.
20. Jayshri, K., A. Desai, and C. Y. D. Sim, "Wideband four-port MIMO antenna array with high isolation for future wireless systems," *AEU — International Journal of Electronics and Communications*, Vol. 128, 153507, 2021.
21. Kang, L., H. Li, X. H. Wang, et al., "Miniaturized band-notched UWB MIMO antenna with high isolation," *Microw. Opt. Technol. Lett.*, Vol. 58, No. 4, 878–881, 2016.
22. Chen, L. Y., J. S. Hong, and M. Amin, "A compact CPW-fed MIMO antenna with band-notched characteristic for UWB system," *ACES Journal*, Vol. 33, No. 7, 818–821, 2018.
23. Chandel, R. and A. K. Gautam, "Compact MIMO/diversity slot antenna for UWB applications with band-notched characteristics," *Electron Lett.*, Vol. 52, 336–338, 2016.
24. Satam, V. and S. Nema, "Dual notched, high gain diversity antenna for wide band applications," *Microw. Opt. Technol. Lett.*, Vol. 59, No. 5, 1222–1226, 2017.
25. Jettia, C. R. and V. R. Nandanavanam, "Trident-shape strip loaded dual band-notched UWB MIMO antenna for portable device applications," *Int.J. Electron. Commun. (AEÜ)*, Vol. 83, 11–21, 2018.
26. Khan, M. I. and M. I. Khattak, "Designing and analyzing a modern MIMO-UWB antenna with a novel stub for stop band characteristics and reduced mutual coupling," *Microw. Opt. Technol. Lett.*, Vol. 62, No. 10, 3209–3214, 2020.
27. Chandel, R., A. K. Gautam, and K. Rambabu, "Tapered fed compact UWB MIMO-diversity antenna with dual band-notched characteristics," *IEEE Trans. Antennas Propag.*, Vol. 66, No. 4, 1677–1684, 2018.
28. Zhao, Y., F. S. Zhang, L. X. Cao, and D. H. Li, "A compact dual band-notched MIMO diversity antenna for UWB wireless applications," *Progress In Electromagnetics Research C*, Vol. 89, 161–169, 2019.
29. Jaglan, N., S. D. Gupta, E. Thakur, et al., "Triple band notched mushroom and uniplanar EBG structures based UWB MIMO/diversity antenna with enhanced wide band isolation," *Int. J. Electron. Commun.(AEÜ)*, Vol. 90, 36–44, 2018.
30. Dalal, P. and S. K. Dhull, "Design of triple band-notched UWB MIMO/diversity antenna using triple bandgap EBG structure," *Progress In Electromagnetics Research C*, Vol. 113, 197–209, 2021.
31. Chen, Z. J., W. S. Zhou, and J. S. Hong, "A miniaturized MIMO antenna with triple band-notched characteristics for UWB applications," *IEEE Access*, Vol. 9, 63646–63655, 2021.
32. Premalatha, B., G. Srikanth, and G. Abhilash, "Design and analysis of multi band notched MIMO antenna for portable UWB applications," *Wireless Personal Communications*, Vol. 118, No. 5, 1697–1708, 2021.
33. Mobashsher, A. T. and A. Abbosh, "Utilizing symmetry of planar ultrawideband antennas of size reduction and enhanced performance," *IEEE Antennas Propag. Mag.*, Vol. 57, No. 2, 153–166, 2015.
34. Yang, B., M. Z. Chen, and L. Y. Li, "Design of a four-element WLAN/LTE/UWB MIMO antenna using half-slot structure," *Int. J. Electron. Commun. (AEÜ)*, Vol. 93, 354–359, 2018.